Trop J Phytochem Pharm Sci, March 2026; 5(2): 468 - 474 **ISSN 2955-1226 (Print)**
ISSN 2955-123(Electronic)

Tropical Journal of Phytochemistry & Pharmaceutical Sciences

Available online at https://www.tjpps.org

Original Research Article

Structure-Based Virtual Screening Identifies Ritobegron and Resveratrol as Dual Inhibitors of NMDA and PTP-1B for Alzheimer's Disease Therapy

Chidinma R Nwizu[1]*, Charles O. Nnadi[1,2], Arnold C. Igboasoiyi[1]

[1]*Department of Pharmaceutical Chemistry, Faculty of Pharmacy, Madonna University, Nigeria, 511101 Elele Campus, Rivers State, Nigeria*
[2]*Department of Pharmaceutical and Medicinal Chemistry, Faculty of Pharmaceutical Sciences, University of Nigeria, Nsukka, Nigeria, 410001 Nsukka, Enugu State, Nigeria*

ABSRTACT

Many Alzheimer's disease (AD) drug candidates fail during clinical translation due to poor target validation and inadequate penetration across the blood–brain barrier. This study aimed to identify potential inhibitors for AD by targeting N-methyl-D-aspartate (NMDA) and protein tyrosine phosphatase 1B (PTP1B). A total of 2,399,743 molecules retrieved from the ChEMBL database were filtered using various *in silico* techniques to identify small, investigational molecules under phase III clinical trial, that are safe, bioavailable with favourable physicochemical properties. The top-ranked molecules were subjected to molecular docking studies on NMDA and PTP1B. A total of 1,920,643 small molecules were identified, among which 1,110 investigational molecules had advanced to phase III clinical trials. Of these, 298 molecules met the Lipinski Rule of Five and were considered safe, and ultimately only 3 molecules demonstrated favourable physicochemical properties. Ritobegron, docked with PTP1B, showed a binding energy, E of -8.69 kcal/mol and an inhibition constant, Ki of 0.424 µM, outperforming the native ligand (-7.23 kcal/mol, 5.04 µM) and with NMDA showed E of -8.06 kcal/mol and Ki of 1.23 µM, both superior to its native ligand (-7.40 kcal/mol, 3.74 µM). Resveratrol, docked with protein PTP1B, showed E of –7.59 kcal/mol and Ki of 2.53 µM, slightly more negative than the native ligand (–7.23 kcal/mol, 5.04 µM). These interactions involved hydrogen bonding, pi-stacking, and hydrophobic interactions with key amino acid residues. The study suggests that ritobegron and resveratrol could serve as promising inhibitors for NMDA receptors and PTP1B enzyme, offering potential therapeutic avenues for AD treatment.

Keywords: Alzheimer's disease, N-methyl-D-aspartate, tyrosine-protein phosphatase, binding affinity, inhibition constant, blood-brain barrier

Received 01 March 2026
Revised 02 April 2026
Accepted 02 April 2026
Published online 10 April 2026

Introduction

Alzheimer's disease (AD) is characterised by the deposition of amyloid protein outside neurons, resulting in the formation of plaques, and inside neurons as neurofibrillary tangles composed of hyperphosphorylated tau protein. These pathological changes lead to synaptic dysfunction, neuronal loss, and progressive cognitive decline. [1] It is the most common cause of dementia and accounts for approximately 60–80 % of all dementia cases worldwide. [2] The exact cause of AD remains unknown, but it is believed to involve a combination of genetic, environmental, and lifestyle factors. [3] Several hypotheses have been proposed to explain the pathogenesis of AD, including the cholinergic hypothesis, amyloid cascade hypothesis, tau hyperphosphorylation hypothesis, metal ion dysregulation, and neuroinflammatory pathways. [1] The hallmark features of AD include the accumulation of β-amyloid plaques and tau tangles in the brain, which result in neuronal damage and subsequent decline in cognitive function. The current burden of AD demands the development of new therapeutic approaches. Globally, AD is a major contributor to disability, mortality, and healthcare costs among older adults, with prevalence increasing sharply with age.

***Corresponding author. mail:** ritaudrey2k18@gmail.com
Tel: +234 906 344 2699

Citation: Nwizu CR, Nnadi CO, Igboasoiyi AC. Structure-Based Virtual Screening Identifies Ritobegron and Resveratrol as Dual Inhibitors of NMDA and PTP-1B for Alzheimer's Disease Therapy. Trop J Phytochem Pharm Sci, 2026, 5(2): 468 - 474
http://www.doi.org/10.26538/tjpps/v5i2.4

Official Journal of Natural Product Research Group, Faculty of Pharmacy, University of Benin, Benin City, Nigeria.

[4] The number of affected individuals is expected to rise further over the coming decades, particularly in low- and middle-income countries. This growing burden highlights the urgent need for disease-modifying therapies rather than treatments that only provide symptomatic relief. [3] At present, there is no cure for AD, and available medications only offer modest symptomatic benefits with limited impact on disease progression. [5]

Virtual screening has become an important tool in modern drug discovery, allowing the rapid identification of compounds with potential biological activity against specific molecular targets. These *in silico* approaches reduce the time and cost associated with traditional experimental screening by predicting ligand–target interactions before *in vitro* and *in vivo* validation. [6]

One approach to developing new treatments for AD is to target specific molecular mechanisms involved in disease progression. Enzymes and receptors such as acetylcholinesterase (AChE), β-secretase (BACE-1), N-methyl-D-aspartate (NMDA) receptors, and protein tyrosine phosphatase 1B (PTP1B) have been implicated in the development of AD. [7] Inhibiting these targets may help to slow or halt disease progression. However, several candidate drugs developed as AChE inhibitors, NMDA receptor antagonists, and Aβ-modulating agents have failed at the clinical trial stage due to limited efficacy or safety concerns. [3] There is increasing evidence that abnormal regulation of protein tyrosine phosphatases, particularly PTP1B, plays a role in the pathogenesis of AD. Overexpression of PTP1B has been associated with cognitive impairment, whereas neuron-specific ablation of PTP1B has been shown to preserve synaptic function and memory. [8] These findings suggest that PTP1B represents a promising therapeutic target for AD drug development.

Despite promising *in vitro* findings, many AD drug candidates fail during clinical translation due to poor target validation, disease-stage dependency, and inadequate penetration across the blood–brain barrier

(BBB). [1] The BBB remains a major challenge in central nervous system drug development, as it restricts the entry of many potentially active compounds into the brain. [5] Consequently, compounds that demonstrate inhibitory activity against targets such as AChE or PTP1B *in vitro* often fail to achieve sufficient brain exposure or meaningful clinical benefit.

In view of these challenges, this study aims to identify investigational compounds with strong predicted affinity for NMDA receptors and PTP1B, while also considering pharmacokinetic properties relevant to BBB permeation. By integrating virtual screening and molecular docking approaches, this work seeks to contribute to the discovery of potential disease-modifying agents for Alzheimer's disease.

Materials and Methods

Chemical datasets

A library of 2,399,743 investigational compounds was collected from a freely accessible chemical database, ChEMBL.[9] The selected compounds comprise different chemical functionalities.

Software and webservers

PreADMET software uses mathematical models and algorithms to simulate the behaviour of drugs in the body and predict their potential side effects and efficacy. The ProTox-II is a virtual laboratory for the prediction of toxicities of small molecules.[10] The Discovery Studio Visualizer was used for analyses and visualisation of interactions. The 3D structures of the target proteins were retrieved from the Protein Data Bank.[11] Autodock4 (v.1.5.6) is a suite of automated docking tools designed to predict how small molecules, such as substrates or drug candidates, bind to a receptor of known 3D structure. [12] Protein-Ligand Interaction Profiler is an online web tool used to identify amino acids of targets that interact with ligands.[13]

Target proteins

The 3D structures of the target proteins, a ligand binding core of the NR1 subunit of the N-methyl-D-aspartate (NMDA) receptor (PDB ID: 1PBQ) and non-receptor subtype 1 protein tyrosine phosphatase 1B (TPP1B) receptor (PDB ID: 4Y14), with resolutions of 1.90 Å each, were retrieved from the Protein Data Bank (PDB) in complex with 5,7-dichlorokynurenic acid (DCKA) and 3-bromo-4-[difluoro(phosphono)methyl]-N-methyl-N-alpha-(methylsulfonyl)-L-phenylalaninamide (DFPM-PAA) respectively. [14,15]

Pretreatment of the dataset

The pretreatment of the chemical dataset followed the flow chart in Figure 1. Small molecules (compounds with MW < 1500 Daltons) that interact with defined biological targets were filtered from the pool of investigational molecules. Further filtration criteria, such as the investigational molecules in phase III clinical trial, drug likeness and non-toxicity were applied.

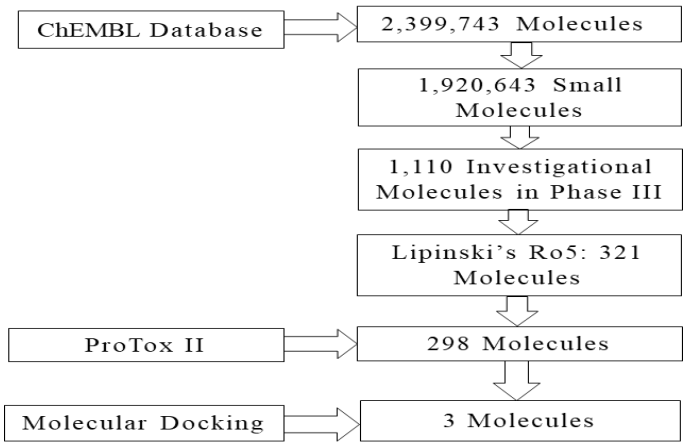

Figure 1: Pretreatment process of the dataset

Prediction of drug likeness

Drug-likeness was assessed using Lipinski's Rule of Five (molecular weight ≤ 500 Da, logP ≤ 5, hydrogen bond donors ≤ 5, acceptors ≤ 10) and topological polar surface area (TPSA) using the SwissADME web server. [16]

Prediction of toxicity endpoints

The toxicity parameters, such as hepatotoxicity, carcinogenicity, immunotoxicity, mutagenicity, and cytotoxicity, were predicted for the compounds that passed Lipinski's RO5 using ProTox-II. [10,17] Compounds that have no toxicity against the target organs and with high LD_{50} (classes 4, 5 or 6 toxicity profile) were selected for further studies. The toxicity cutoff was placed at toxicity classes of at least 4.

Preparation of target proteins

The protein structures were prepared by removing water molecules and other non-amino acid units such as cofactors, metals, ligand and heteroatoms. The missing atoms or residues were detected, repaired, and their geometry optimised. The polar hydrogens and Kollman charges were assigned, and force field parameters were generated for the proteins using Autodock 1.5.6. [18]

Preparation of ligands and setting grid parameters

The ligand was loaded in the Autodock window, the root was detected, and the number of torsions was set to the default. The grid parameters were set to reflect the blind docking protocol with specified centre coordinates of x = 19.8, y = 27.6 and z = 39.1 in their respective grid box of 60 Å dimensions each for 1PBQ and centre coordinates of x = 12.5, y = 24.3 and z = 44.6 in their respective grid box of 60 Å dimensions each for 4Y14. The Autogrid was run using the Autogrid4 programme. [19]

Preparation of docking parameters

The pdbqt file of the protein and the ligand were reloaded in the Autodock programme. The docking parameters were created using the genetic algorithm programme. The programme adopted a setting of the number of GA runs (50) and population size of 300, and other parameters were defaulted. [20]

Molecular docking of hit compounds

The three selected compounds were subjected to a molecular docking study on the selected targets. The target validation was established by re-docking the co-crystallised ligands to obtain RMSD < 2.0Å. The docking protocol followed a blind technique using the Autodock4 programme and default settings. [12]

Analysis of docking results

The interactions of the ligands with the binding pockets of the proteins were evaluated using the inhibition constants and binding energies, while the properties of the ligand pose in the active site residues were visualised using the Discovery Studio Visualizer (DSV) software and the Protein-Ligand Interaction Profiler web server. [13] The amino acids responsible for the different interactions formed from the docked ligands, as well as the interaction distances, were recorded.

Results and Discussion

Ligand library screening

Three investigational compounds, resveratrol, ritobegron and transcrocetin were ranked the safest and drug-like from the 2,399,743 compounds obtained from the ChEMBL database (Figure 2).

Predicted toxicities of hit compounds

The molecules were checked for their oral acute toxicity, hepatotoxicity, carcinogenicity, immunotoxicity, mutagenicity, and cytotoxicity activities using the ProToxII webserver. The results are

indicated in Table 1. Three small molecules, B, C and A, were initially considered safe based on ProTox II criteria. [10] However, oral acute toxicity predictions categorised the molecules in classes IV and V, highlighting the need for experimental validation. Despite this, all three compounds demonstrated high intestinal absorption. Resveratrol and trans-resveratrol exhibited strong plasma protein binding, a property of considerable pharmacological importance. Protein binding enhances stability, solubility, and circulation time, thereby increasing therapeutic potential, since these compounds are otherwise prone to enzymatic degradation and rapid elimination. [21] Previous studies have shown that resveratrol binds to albumin, alpha-1 glycoprotein, and low-density lipoprotein. [22] Albumin, with its high binding capacity, forms large complexes that limit passive diffusion across the blood–brain barrier. [23] In contrast, alpha-1 glycoprotein has a relatively small binding site and limited ligand accommodation.

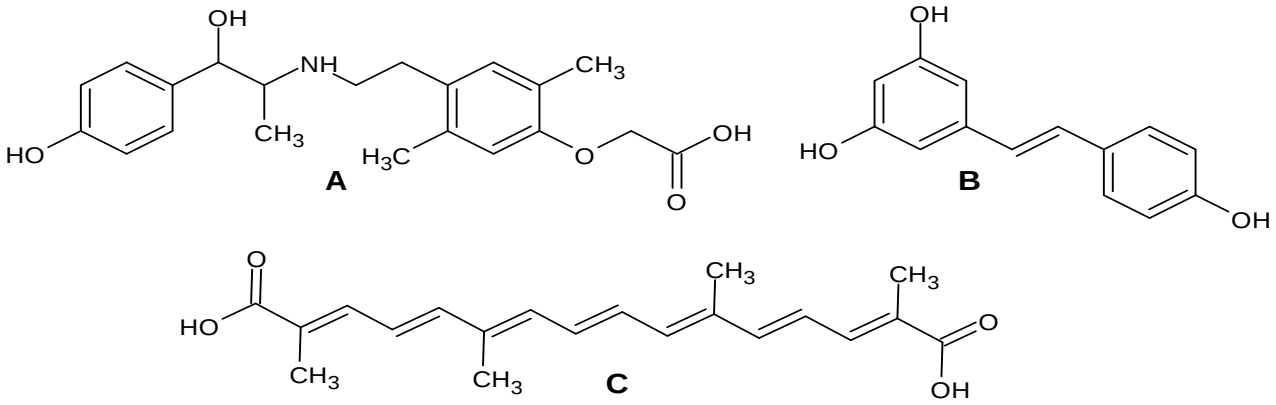

Figure 2: Investigational hit compounds identified from various treatments (**A** = ritobegron; **B** = resveratrol, and **C** = transcrocetin)

Table 1: Toxicity profiles of the hit compounds

Ligands	**LD_{50}** (mg/kg), **Class**	**Hepat**	**Carcin**	**Immun**	**Mutag**	**Cytotox**
A	1580, IV	I – 0.94	I – 0.70	I – 0.82	I – 0.73	I – 0.71
B	1560, IV	I – 0.74	I – 0.71	I – 0.86	I – 0.92	I – 0.98
C	4300, V	I – 0.72	I – 0.74	I – 0.99	I – 0.72	I – 0.72

A (ritobegron), B (resveratrol), C (transcrocetin), Hepatotoxicity (Hepat), carcinogenicity (Carcin), immunotoxicity (Immun), mutagenicity (Mutag), cytotoxicity (Cytotox). Toxicity classes are defined according to the globally harmonised system of classification and labelling of chemicals (GHS). LD_{50} values are given in (mg/kg): Class IV: harmful if swallowed ($300 < LD_{50} \leq 2000$), Class V: may be harmful if swallowed ($2000 < LD_{50} \leq 5000$), Class VI: non-toxic ($LD_{50} > 5000$). I – inactive
Below 0.70 → Low confidence
The closer the value is to 1, the more reliable the prediction.

Pharmacokinetic properties of hit compounds

The ADME parameters include absorption (intestinal absorption), distribution (BBB permeation), metabolism (CYP2C9 inhibitor, CYP3A4 substrate, CYP3A4 inhibitor, CYP2C19 inhibitor, CYP2D6 substrate and CYP2D6 inhibitor), but the excretion parameters were not applicable. The result is shown in Table 2. Age-related changes further influence binding dynamics: serum albumin levels decline with age, reducing resveratrol binding and brain penetration, while alpha-1 glycoprotein levels increase, expanding available binding sites and potentially facilitating resveratrol's penetration into the brain. Ritobegron, by contrast, was only weakly bound to plasma proteins. [24] This results in a larger fraction of the drug remaining unbound and pharmacologically active, contributing to a shorter half-life. Such a profile can be advantageous, offering dosing flexibility, minimising accumulation, and reducing risks of drug–drug displacement interactions. [21] Metabolic profiling revealed that all three compounds were inhibitors of CYP3A4 but not substrates of CYP2D6. Resveratrol was unique in being neither a substrate of CYP3A4 nor an inhibitor of CYP2C9. Ritobegron alone inhibited CYP2D6, while transcrocetin selectively inhibited CYP2C19.

Molecular docking studies

The molecular docking of each protein with its respective ligands was performed. The binding energy and the inhibition constant, as well as the amino acids responsible for the different interactions, which include hydrogen bonding, hydrophobicity, pi-stacking, salt bridge, and halogen bonding, were noted, along with the bond distances. The results are shown in Tables 3 and 4, with the molecular visualisations of these interactions shown in Figures 3 and 4.

Interaction of hit compounds with the NMDA target

The interaction of the identified compounds with the NMDA receptor showed that A elicited the strongest interaction with the target, higher than the negative ligand, when compared with ligands B and C (Table 3). Several amino acids of NMDA were involved in the H bond, hydrophobic, and π– stacking interactions of A, including PHE246A, THR126A, ARG131A, VAL181A, GLN144A, SER180A for hydrogen bonding as well as ASP224A, TRP223A, VAL181A, LEU146A, GLN144A for hydrophobic interactions (Figure 3Aa, b and c).

Interaction of hit compounds with TPP1B target

The interaction of the identified compounds with the TPP1B receptor showed that A elicited the strongest interaction with the target, higher than the negative ligand, when compared with ligands B and C (Table 4). Ligand B (E = - 7.59 kCal/mol) also showed a stronger interaction than the co-crystalised ligand (E = -7.23 kCal/mol). Several amino acids of TPP1B were involved in the H bond, and hydrophobic interactions of A, including GLU75A, GLN78A, ARG79A and SER80A for hydrogen bonding as well as LYS73A, GLN78A, ARG79A, LEU204A and PRO 206A for hydrophobic interactions (Figure 4Aa, b and c).

ISSN 2955-1226 (Print)
ISSN 2955-123(Electronic)

Table 2: Pharmacokinetics of hit compounds

Pharmacokinetics	A (ritobegron)	B (resveratrol)	C (transcrocetin)
Absorption (%)	90.18	88.479	96.708
Distribution (%)	72.18	100.0	94.836
BBB Permeation	0.365	1.738	1.0890
CYP 3A4 substrate	Substrate	None	Substrate
CYP 3A4 inhibition	Inhibitor	Inhibitor	Inhibitor
CYP 2D6 substrate	None	None	None
CYP 2D6 inhibition	Inhibitor	None	None
CYP 2C9 inhibition	Inhibitor	None	Inhibitor
CYP 2C19 inhibition	None	None	Inhibitor

BBB permeation is measured as LogBB (logarithm of brain-to-blood concentration ratio), CYP = cytochrome P.

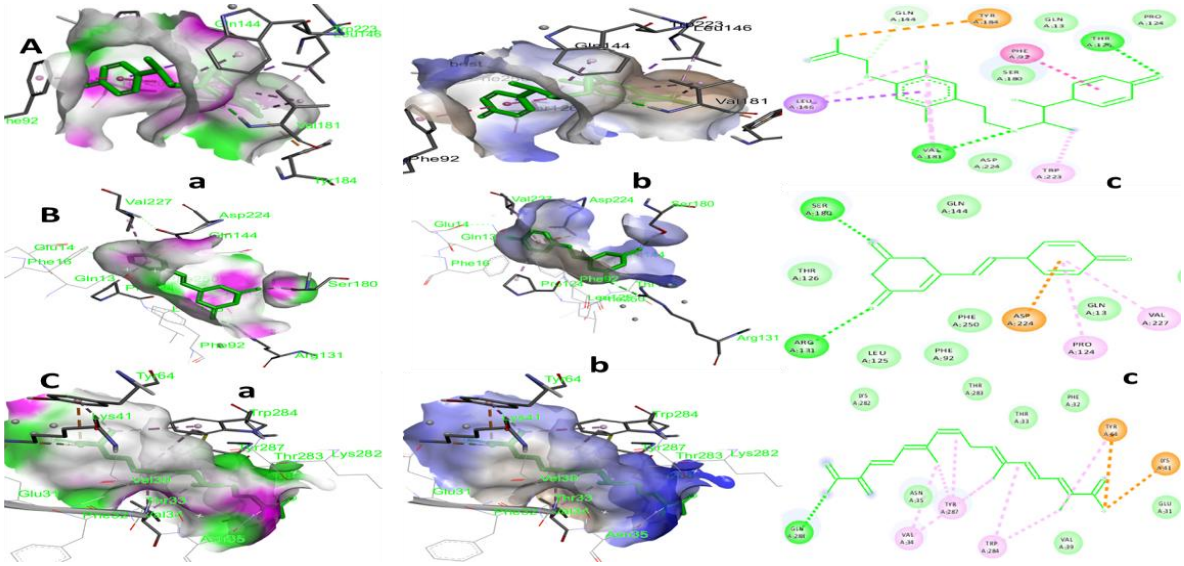

Figure 3: Best docked poses showing the interactions between the specific amino acids of the NMDA receptor and hit compounds A, B and C. (a = 3D surface hydrogen bond interactions, b = 3D surface hydrophobic interaction and c = 2D interactions)

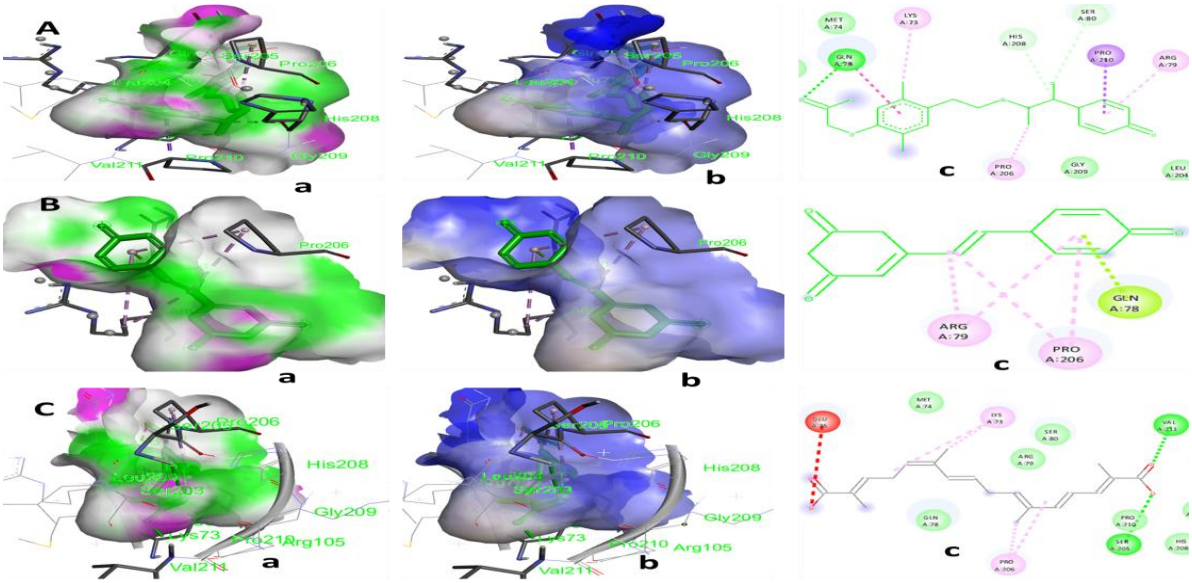

Figure 4: Best docked poses showing the interactions between the specific amino acids of the TPP1B receptor and hit compounds A, B and C. (a = 3D surface hydrogen bond interactions, b = 3D surface hydrophobic interaction and c = 2D interactions)

ISSN 2955-1226 (Print)
ISSN 2955-123(Electronic)

Table 3: Binding parameters of protein NMDA docked with hit compounds.

Compounds	E (kcal/mol)	Ki (μM)	Interactions
DCKA	- 7.40	3.74	H bond, hydrophobic, π– stacking, salt bridge
A	-8.06	1.23	H bond, hydrophobic, π– stacking
B	- 6.97	7.77	H bond, hydrophobic, π– stacking
C	- 6.66	13.18	H bond, hydrophobic, salt bridge

Table 4. Binding parameters of protein PTP1B docked with hit compounds.

Compounds	E (kcal/mol)	Ki (μM)	Interactions
DFPM-PAA	-7.23	5.04	H bond, hydrophobic, halogen bond
A	- 8.69	0.424	H bond, hydrophobic
B	- 7.59	2.73	H bond, hydrophobic
C	- 7.19	5.34	H bond, hydrophobic

Ligands with lower (more negative) binding energies generally exhibit stronger interactions with their target proteins, while lower inhibition constants indicate higher ligand affinity. [25] Moreover, the binding between a native ligand and its receptor (protein or enzyme) is typically highly specific and of high affinity. Thus, comparing native ligands with other ligands provides a useful benchmark for validating the accuracy of molecular docking results. [12] Based on the docking analysis, the top-ranked interaction was between protein PTP1B and compound A, which showed a binding energy of –8.69 kcal/mol, more negative than that of the native ligand (–7.23 kcal/mol). Correspondingly, the inhibition constant for PTP1B docked with A was 0.424 μM, markedly lower than the native ligand's 5.04 μM, indicating stronger binding affinity.

The second-ranked interaction involved protein NMDA docked with compound A, yielding a binding energy of –8.06 kcal/mol, again more negative than the native ligand's –7.40 kcal/mol. The inhibition constant for NMDA docked with A was 1.23 μM, compared to 3.74 μM for the native ligand, further supporting enhanced affinity. The third-ranked interaction was observed between protein PTP1B and B, with a binding energy of –7.59 kcal/mol, slightly more negative than the native ligand's –7.23 kcal/mol. The inhibition constant for PTP1B docked with B was 2.73 μM, lower than the native ligand's 5.04 μM, again suggesting improved binding affinity.

Ligand A docked with protein PTP1B revealed several amino acids responsible for hydrogen bonding and hydrophobic interactions. The residues involved in hydrogen bonding were GLU75A, GLN78A, ARG79A, and SER180A. Specifically, the carbonyl oxygen (C=O) of glutamic acid (GLU75A) interacted with the OH group of A, while the NH_2 group of glutamine (GLN78A) formed a hydrogen bond with the OH group of A. The guanidinium group of arginine (ARG79A) interacted with the OH group at the 4th carbon atom of phenyl ring A of molecule A, and the OH group of serine (SER180A) formed a hydrogen bond with the OH group of ritobegron. Hydrophobic interactions were mediated by LYS73A, GLN78A, ARG79A, LEU204A, and PRO206A. The CH_2 group of lysine (LYS73A) interacted with the 2nd carbon atom of phenyl ring B of A (bearing CH_3 groups at the 2nd and 5th positions). The CH_2 group of glutamine (GLN78A) bonded to the CH_3 group at the 5th carbon atom of phenyl ring B of ritobegron. The CH_2 group of arginine (ARG79A) at the 3rd carbon atom interacted with the CH_2 group at the 5th carbon atom of phenyl ring A of A (bearing an OH group at the 4th carbon atom). The α-carbon of leucine (LEU204A) bonded to the CH_2 group at the 3rd carbon atom of phenyl ring A of A, while the CH_2 group of the five-membered ring of proline (PRO206A) bonded to the CH_3 group of A.

Ligand A docked with protein NMDA showed amino acids responsible for hydrogen bonding, hydrophobic interactions, and π-stacking. The hydrogen-bonding residues included PHE246A, THR126A, ARG131A, GLN144A, and SER180A. The carbonyl oxygen of phenylalanine (PHE246A) interacted with the OH group at the 9th carbon atom of phenyl ring A of molecule A. The α-carbon hydrogen of threonine (THR126A) formed a hydrogen bond with the OH group at the 4th carbon atom of phenyl ring A of molecule A. The guanidinium group of arginine (ARG131A) interacted with the OH group at the 4th carbon atom of phenyl ring A of ritobegron. Additionally, the NH_2 group of valine (VAL181A) interacted with the NH group of A, while serine (SER180A) formed multiple hydrogen bonds with both the NH and OH groups of A. Glutamine (GLN144A) also interacted with the OH group of A. π-stacking interactions were observed with phenylalanine (PHE92A), where the aromatic ring of PHE92A stacked against the phenyl ring A of molecule A (bearing an OH group at the 4th carbon atom).

According to the protein–ligand interaction profiler, the maximum donor–acceptor distance for hydrogen bonding is ≤ 4.1 Å, while the maximum carbon–carbon distance for hydrophobic interactions is ≤ 4.0 Å. [13] Importantly, shorter hydrogen bond distances correlate with stronger interactions and improved binding affinity. All hydrogen bonding and hydrophobic interactions observed for ligand A fell within these acceptable ranges, supporting the stability and validity of the docking results.

Memantine remains the reference NMDA receptor antagonist with moderate affinity, exhibiting binding energies of approximately –7.5 kcal/mol and inhibition constants (Ki) in the range of 0.5–1 μM. This moderate affinity is sufficient for clinical efficacy with a favourable safety profile. In contrast, ketamine derivatives demonstrate stronger binding (–8 to –9 kcal/mol) and lower Ki values (~0.2–0.5 μM), but their therapeutic use in Alzheimer's disease is constrained by adverse psychotropic effects and limited tolerability. [26] For PTP1B inhibition, synthetic inhibitors such as trodusquemine and benzofuran derivatives exhibit high potency, with binding energies between –9 and –11 kcal/mol and Ki values in the nanomolar range (20–200 nM). These compounds selectively block PTP1B, thereby enhancing insulin and leptin signalling, pathways implicated in neurodegeneration. By comparison, resveratrol, a natural polyphenol, shows weaker activity with binding energies of –6 to –7 kcal/mol and Ki values in the micromolar range (20–50 μM). Although limited by poor bioavailability, resveratrol provides additional antioxidant and anti-inflammatory benefits that may contribute to neuroprotection. 27

Conclusion

The findings of this study demonstrate that virtual screening is a reliable approach for identifying potential inhibitors of key targets implicated in Alzheimer's disease, specifically NMDA receptors and the tyrosine-protein phosphatase enzyme (PTP1B). Among the screened compounds, ritobegron and resveratrol exhibited superior binding affinities and lower inhibition constants compared to their respective native ligands, underscoring their promise as lead candidates. These results not only validate the effectiveness of computational docking in drug discovery but also highlight ritobegron

and resveratrol as strong therapeutic contenders that warrant further experimental evaluation for the development of novel Alzheimer's disease treatments.

Conflicts of interest

The author declares no conflicts of interest

Authors' Declaration

The authors hereby declare that the work presented in this article is original and that any liability for claims relating to the content of this article will be borne by them.

.

References

1. Frisoni GB, Aho E, Brayne C, Ciccarelli O, Dubois B, Fox NC, Frederiksen KS, Gabay C, Garibotto V, Hofmarcher T, Jack CR. Alzheimer's disease outlook: controversies and future directions. The Lancet. 2025; 406(10510): 1424-1442. https://doi.org/10.1016/S0140-6736(25)01389-3.
2. Rahman A, Jaiswal A, Keshari P, Singh DK. Alzheimer's: Epidemiology, pathophysiology, diagnosis, and treatments. In Proteostasis: Investigating molecular dynamics in neurodegenerative disorders 2025; 39-72. Singapore: Springer Nature Singapore. https://doi.org/10.1007/978-981-96-6202-9_2
3. Cummings J, Lee G, Nahed A, Kambar MEN, Zhong K, Fonseca J, Taghva K. Alzheimer's disease drug development pipeline: 2022. Alzheimers Dement (NY). 2022; 8(1): e12295. https://doi.org/10.1002/trc2.12295
4. Scheltens P, De Strooper B, Kivipelto M, Holstege H, Chételat G, Teunissen CE, Cummings J, van der Flier WM. Alzheimer's disease. The Lancet. 2021; 397(10284): 1577-1590. https://doi.org/10.1016/s0140-6736(20)32205-4
5. Xing H, Yue S, Qin R, Du X, Wu Y, Zhangsun D, Luo S. Recent advances in drug development for Alzheimer's disease: A Comprehensive Review. Int J Mol Sci. 2025; 26(8): 3905. https://doi.org/10.3390/ijms26083905
6. Hossain MS, Hussain MH. Multi-target drug design in Alzheimer's disease treatment: emerging technologies, advantages, challenges, and limitations. Pharmacol Res Perspect. 2025; 13(4): e70131. https://doi.org/10.1002/prp2.70131
17. alkaloids from the Toxic Plants-Phytotoxins database. Trop J Phytochem Pharm Sci. 2025; 4(2): 68-72. https://doi.org/10.26538/tjpps/v4i2.6
18. Nnadi CO, Ozioko LU, Eneje GC, Onah CM, Obonga WO. *In-vivo* antitrypanosomal effect and in-silico prediction of chronic toxicity of *N*-methylholaphyllamine in rats. Trop J Pharm Res. 2020; 19(11): 2369-2375. https://doi.org/10.4314/tjpr.v19i11.18
19. Nnadi CO, Onuku RS, Ayoka TO, Okorie HN, Nwodo NJ. Chemical constituents of *Combretum dolichopetalum*: Characterisation, antitrypanosomal activities and molecular docking studies. Trop J Pharm Res. 2022; 21(4): 801-808. https://doi.org/10.4314/tjpr.v21i4.17
20. Nnadi CO, Ngwu SO, Ohagwu MBZ. *In-vivo* and *in-silico* evidence of antitrypanocidal activities of selected plants from the Asteraceae family against *Trypanosoma brucei brucei*. Bioint Res Appl Chem. 2023; 13(1): 30. https://doi.org/10.33263/BRIAC131.030
21. Ezema IF, Akwu VC, Didigwu OK, Ogbonna JE, Ugwu AC, Nnadi CO. Exploring different drug targets responsible for the inhibitory activity of N, N'-substituted diamine derivative in Leishmania. Eng Proc. 2023; 56(1): 178. https://doi.org/10.3390/ASEC2023-16264
7. Zaki SB, Khan SA, Ali R. A multi-enzyme study reviewing the role of target enzymes in Alzheimer's disease and unveiling potential inhibitors with insights on their present and future assessment. Med Chem Res. 2025; 34(3): 549-570. https://doi.org/10.1007/s00044-025-03373-w.
8. Kołodziej-Sobczak D, Sobczak Ł, Łączkowski KZ. Protein tyrosine phosphatase 1B (PTP1B): A comprehensive review of its role in pathogenesis of human diseases. Int J Mol Sci. 2024; 25(13): 7033. https://doi.org/10.3390/ijms25137033
9. Mendez D, Gaulton A, Bento AP, Chambers J, De Veij M, Félix E, Magariños MP, Mosquera JF, Mutowo P, Nowotka M, Gordillo-Marañón M. ChEMBL: towards direct deposition of bioassay data. Nucleic acids Res. 2019; 47(D1): D930-D940. https://doi.org/10.1093/nar/gky1075
10. Banerjee P, Eckert OA, Schrey AK, Preissner R. ProTox-II: A webserver for the prediction of toxicity of chemicals. Nucleic Acids Res. 2018; 46(W1); W257–W263. https://doi.org/10.1093/nar/gky318
11. Berman HM, Westbrook J, Feng Z, Gilliland G, Bhat TN, Weissig H, Shindyalov IN, Bourne PE. The Protein Data Bank. Nucleic Acids Res. 2000; 28(1): 235–242. https://doi.org/10.1093/nar/28.1.235
12. Morris GM, Huey R, Lindstrom W, Sanner MF, Belew RK, Goodsell DS, Olson AJ. AutoDock4 and AutoDockTools4: Automated docking with selective receptor flexibility. J Comput Chem. 2009; 30(16): 2785-2791. https://doi.org/10.1002/jcc.21256
13. Adasme MF, Linnemann KL, Bolz SN, Kaiser F, Salentin S, Haupt VJ, Schroeder M. PLIP 2021: Expanding the scope of the protein–ligand interaction profiler to DNA and RNA. Nucleic Acids Res. 2021; 49(W1): W530–W534. https://doi.org/10.1093/nar/gkab294
14. Furukawa H, Gouaux E. Mechanisms of activation, inhibition and specificity: crystal structures of the NMDA receptor NR1 ligand-binding core. The EMBO J. 2003; 22(12): 2873–2885. https://doi.org/10.1093/emboj/cdg303
15. Krishnan N, Krishnan K, Connors CR, Choy MS, Page R, Peti W, Van Aelst L, Shea SD, Tonks NK. PTP1B inhibition suggests a therapeutic strategy for Rett syndrome. The J Clin Investig. 2015; 125(8): 3163-3177. https://doi.org/10.1172/jci80323
16. Banda SH, Uzonwanne MU, Didigwu OK, Nnadi CO. Cancer stem cells as potential targets of phytotoxic
22. Smith DA, Beaumont K, Maurer TS, Di L. Relevance of half-life in drug design: Miniperspective. J Med Chem. 2017; 61(10): 4273-4282. https://doi.org/10.1021/acs.jmedchem.7b00969
23. Cottart CH, Nivet-Antoine V, Laguillier-Morizot C, Beaudeux JL. Resveratrol bioavailability and toxicity in humans. Mol Nutr Food Res, 2010; 54(1): 7–16. https://doi.org/10.1002/mnfr.200900437
24. Banks WA. From blood–brain barrier to blood–brain interface: New opportunities for CNS drug delivery. Nature Rev Drug Discov. 2016; 15(4): 275–292. https://doi.org/10.1038/nrd.2015.21
25. Abe Y, Nakano Y, Kanazawa T, Furihata T, Endo T, Kobayashi M. Investigation of drug–drug interactions between ritobegron, a selective β3-adrenoceptor agonist, with probenecid in healthy men. Clin Pharmacol Drug Dev. 2016; 5(3): 201-207. https://doi.org/10.1002/cpdd.212.
26. Agnihotry S, Pathak RK, Srivastav A, Shukla PK, Gautam B. Molecular docking and structure-based drug design. In Computer-aided drug design 2020; 115-131. Singapore: Springer Singapore. https://doi.org/10.1007/978-981-15-6815-2_6

ISSN 2955-1226 (Print)
ISSN 2955-123(Electronic)

27. Podkowa K, Czarnacki K, Borończyk A, Borończyk M, Paprocka J. The NMDA receptor antagonists memantine and ketamine as anti-migraine agents. Naunyn-Schmiedeberg's Archiv Pharmacol. 2023; 396(7): 1371-1398. https://doi.org/10.1007/s00210-023-02444-2
28. Ye S, Han Y, Wei Z, Li J. Binding Affinity and Mechanisms of Potential Antidepressants Targeting Human NMDA Receptors. Molecules. 2023; 28(11):4346. https://doi.org/10.3390/molecules28114346